MAUSAM, 49, 1 (January 1998), 79-94

551.553.21:551.58

A view of global monsoons in observed and model climatology

K.R. SAHA*, HUUG M. VAN DEN DOOL and SURANJANA SAHA

National Centers for Environmental Prediction (NCEP), USA

(Received 6 July 1995, Modified 7 March 1997)

सार — राष्ट्रीय पर्यावरण पूर्वानुमान केन्द्रों (एन. सी. ई. पी.) के भूमंडलीय स्पैक्ट्रल प्रचालन निदर्श के T 62/28 -लेवल वर्जन से प्राप्त हुए 17 वर्षों (1979-1995) के जनवरी से जुलाई के जलवायु विज्ञान संबंधी औसत की उसके पुनः विश्लेषित परियोजना से प्राप्त हुए इसी अवधि के प्रेक्षित जलवायु विज्ञान संबंधी औसतों के साथ तुलना की गई है। इसका उद्देश्य इस तथ्य का पता लगाना है कि सूर्य द्वारा भूमध्य रेखा के साथ वर्ष में इसकी विभिन्न स्थितियों के दौरान पृथ्वी के धरातल पर ऋतुओं के अनुसार विभिन्न स्थानों पर विभिन्न मात्रा में ताप पहुंचाने के बावजूद भी भूमंडलीय मानसून वर्षा के वितरण के कुछ सुपरिचित लक्षणों को यह कितने सही ढंग से आत्मसात कर लेता है। परिसंचरण और वर्षा के कुछ अपवादों को छोड़कर सतह तापमान, सतह दाब, वायुमंडलीय परिसंचरण और भूमंडल के अधिकांश भागोंके कुल वर्षा से संबंधित औसत मासिक विसंगति (वार्षिक माध्य से मासिक माध्य में विचलन) के क्षेत्र में इन दोनों के मध्य काफी अनुकूलता पाई गई है।

मॉडल और प्रेक्षित जलवायु विज्ञान में स्थल महासागर संरूपण, महासागर की शीत और उष्ण सतह तथा उच्च पर्वत श्रृंखलाओं के परिणामस्वरूप विभिन्न क्षेत्रों में मानसून के वितरण और तीव्रता में व्यापक रूप से विविधता के परिलक्षित होने का आभास मिलता है। तथापि, एक गोलार्द्ध से दूसरे गोलार्द्ध तक जाने वाली एकल भूमध्यरेखीय द्रोणी, जो कि मानसून वर्षा के आने तथा उसके आरम्भ होने का कारण है, की संकल्पना विशेष रूप से उष्ण महासागरों के ऊपर, जहाँ दो द्रोणियों के होने के प्रमाण मिलते हैं, मिथ्या प्रतीत होती है। भूमध्यरेखीय द्रोणी ग्रीष्म गोलार्द्ध में मानसून का कारण है। मुख्य महाद्वीपों और महासागरों के बीच मानसून के पूर्व से पश्चिम की ओर चलने के संकेत मिले हैं।

ABSTRACT. A 17-year (1979-95) mean January and July climatology obtained from a T 62/ 28 - level version of the National Centers for Environmental Prediction (NCEP) global spectral operational model is compared with a mean observed climatology for the same period obtained from its reanalysis project, with a view to finding out how well it captures some of the well-known characteristics of the global monsoon circulation generated seasonally by differential heating of the earth's surface by the sun in the course of its annual oscillation about the equator. Good correspondence between the two is found in the fields of mean monthly anomaly (deviation of monthly mean from the annual mean) of surface temperature, surface pressure, atmospheric circulation and total rainfall over most parts of the globe, barring a few exceptions mostly in circulation and rainfall.

Large diversity in the distribution and intensity of monsoon found over different regions due to land-sea configurations, cold and warm ocean surfaces and high mountain ranges appears to be well reflected in model and observed climatology. However, the concept of a single equatorial trough moving from one hemisphere to the other to cause advance and onset of monsoon appears to fail especially over warm oceans, where there appears to be evidence in favour of two troughs, one in each hemisphere. It is the equatorial trough in the summer hemisphere that moves to bring up the monsoon in that hemisphere. There appears to be some evidence to suggest an east-west movement of monsoons between major continents and oceans.

Key words — Global monsoons, Model monsoon climatology, Observed monsoon climatology, Equatorial trough movement.

* *Present affiliation* : 27, B-Road, Maharani Bagh, New Delhi-110065, India

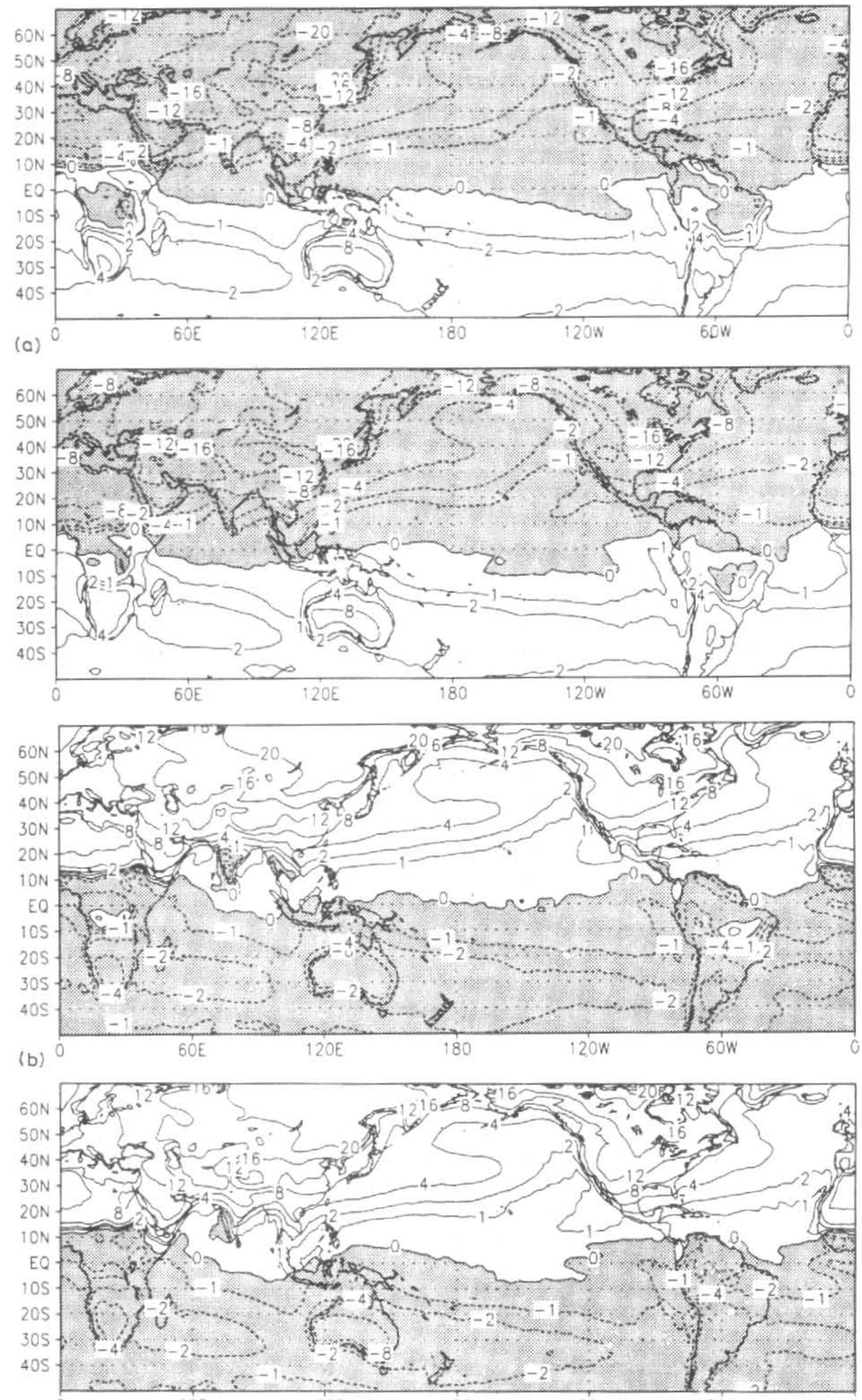

Figs.1 (a&b). Global distributions of observed (reanalysis) and model surface temperature (°C) anomaly (deviation of monthly mean from annual mean) during (a) January and (b) July. Negative anomalies are shaded

1. Introduction

Monsoons form an integral part of the general circulation of the earth's atmosphere. Guided by horizontal pressure gradient, created by differential heating of the earth's surface, such as that between the summer and the winter hemispheres or between a continent and a neighbouring ocean by the sun in the course of its annual oscillation about the equator, these wind systems blow so as to remove excess heat from the warmer to the cooler region via a two-fold circulation, *viz*., a primary horizontal circulation and a secondary vertical circulation which together have come to be known as monsoon circulation. In a typical monsoon circulation, low-level winds from the cooler region blow in a cyclonic circulation around a 'heat low' situated over the warmer region and converge there at a trough of low pressure (associated with the 'heat low') which is generally known as the Equatorial Trough (ET) or the Intertropical Convergence Zone (ITCZ). At the equatorial trough, convergence leads to rising motion. However, due to reversal of the horizontal pressure gradient with height, winds in the middle and upper troposphere blow in an anticyclonic circulation around a 'warm high' and diverge towards the cooler region where they subside. If the air converging at the equatorial trough at low levels and diverging aloft is moist, the rising motion leads to clouding and precipitation at the trough zone. Summer monsoon rainfall is thus typically associated with the ET or the ITCZ. Its seasonal movement between continents and oceans following the annual movement of the sun across the equator is what causes the onset and withdrawal of monsoon at a place.

The above description of a monsoon circulation must, however, be regarded as highly idealized, since, on the real earth, several factors such as geographical location, lead-sea configuration, extensive warm and cold ocean surfaces, high mountain ranges, etc., acting singly or jointly, may introduce significant deviations from the idealized structure. In several regions, depending upon the distributions of land and sea, differential heating may occur not only in the meridional direction but also in the zonal direction. In such regions, the orientation of the equatorial trough may be inclined to both the directions. Over extensive parts of the globe, powerful ocean currents maintain warm or cold surfaces which interfere with the normal location and movement of the equatorial trough. Also, high mountain ranges over some parts of the globe distort the basic structure of the monsoon. Yet another factor which affects the structure and activity of the monsoon in any region is its frequent interaction with extra-tropical disturbances.

For several decades in the past (some references appear in Ramage 1971), scientists looked for monsoon in extra-tropical latitudes where large continents are flanked by still larger oceans. Krishnamurti (1971) and Krishnamurti *et al.* (1973) reviewed the question and discussed the possibility of existence of an east- west vertical circulation between the Asian continent and the Pacific Ocean. Also, a recent study (Van Den Dool and Saha 1993) shows that the seasonal redistribution of atmospheric mass between the Eurasian continent and its surrounding oceans occurs through vertical overturnings not only in the north-south direction but also in the east-west direction.

The objective of the present study is to examine how well a state-of-the -art global circulation model can simulate some of the above-mentioned features of monsoon circulation when integrated over a long period of time. For this purpose, the model climatology will be compared with a climatology obtained from actual observations averaged over the same period through a special analysis scheme known as 'Reanalysis'. A brief introduction to the model and the reanalysis scheme is furnished in section 2.

2. Model and observed climatology

The model climatology used in the present study is obtained by integrating a T62/28-level (horizontal resolution about 210 km, 28 levels in vertical) version of the global spectral model used operationally (1996) at the National Centers for Environmental Prediction (NCEP) in Washington, D.C., USA, for 17 years, using observed sea surface temperatures, snow cover and sea-ice concentrations from 1979 to 1995 as boundary conditions. The model includes parameterization of all major physical processes, *i.e.*, deep convection based on a simplified Arakawa-Schubert convective parameterization scheme developed by Pan and Wu (1994) based on Grell (1993), large-scale precipitation, shallow convection, gravity wave drag, radiation with diurnal cycle and interaction with clouds, boundary layer physics, an interactive surface hydrology and vertical and horizontal diffusion processes. Details of the model physics and dynamics are described in National Oceanic and Atmospheric Administration/National Meteorological Center (NOAA/NMC) Development Division Model Documentation (1988), Kanamitsu (1989) and Kanamitsu *et al.* (1991).

The observed climatology with which the model climatology will be compared is obtained from NCEP/NCAR (National Center for Atmospheric Research) reanalysis project, details of which may be found in Kalnay *et al.* (1996). The project uses a frozen state-of-the-art global data assimilation system and an enhanced database with many sources of observations not available in real time for operations. Rainfall data obtained from reanalysis is for period 1979 to 1992, processed by J.-K.E. Schemm of NCEP, who combined the World surface station rainfall climatology with

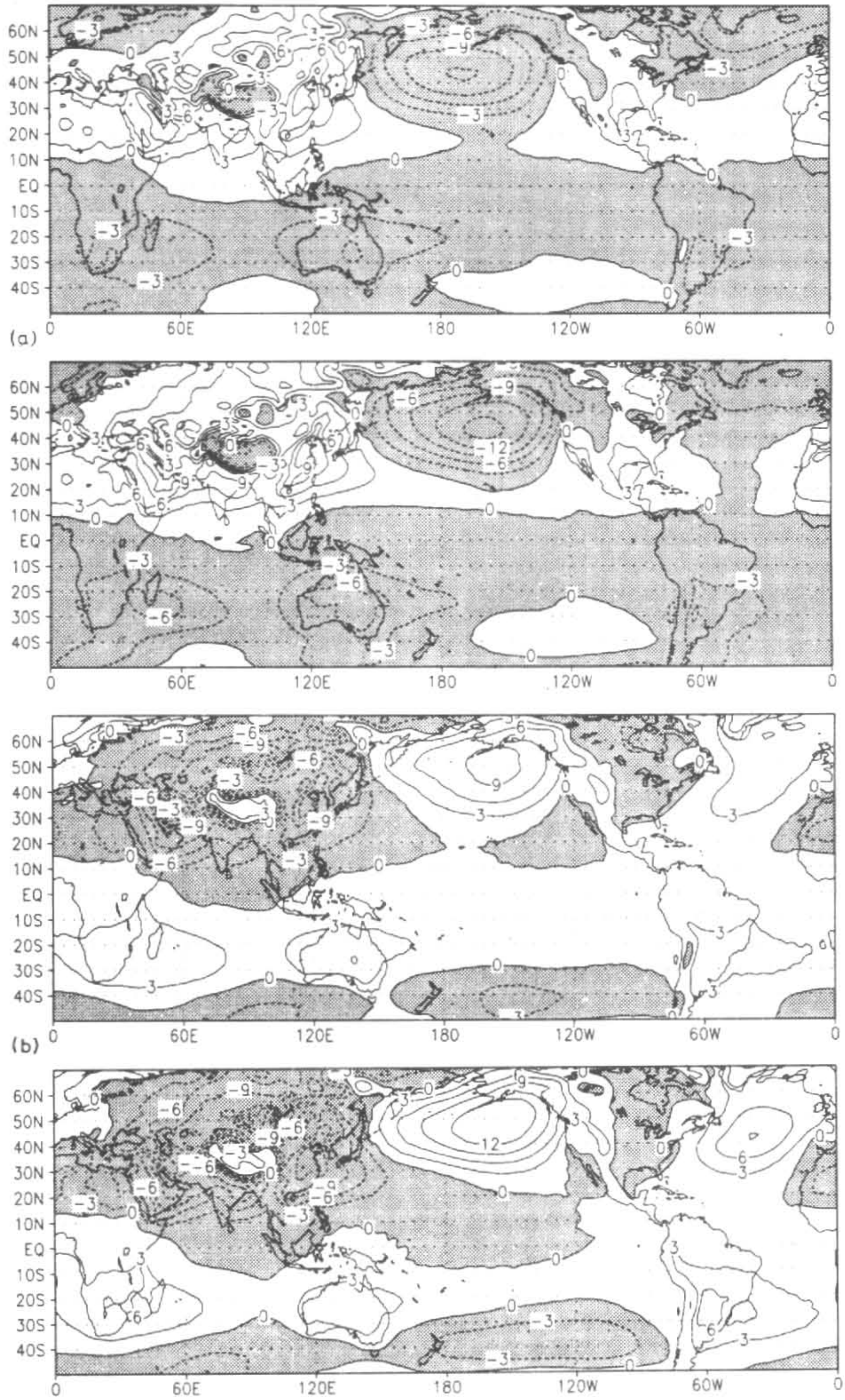

Figs.2(a&b). Same as in Fig.1 but for surface pressure (hPa) anomaly

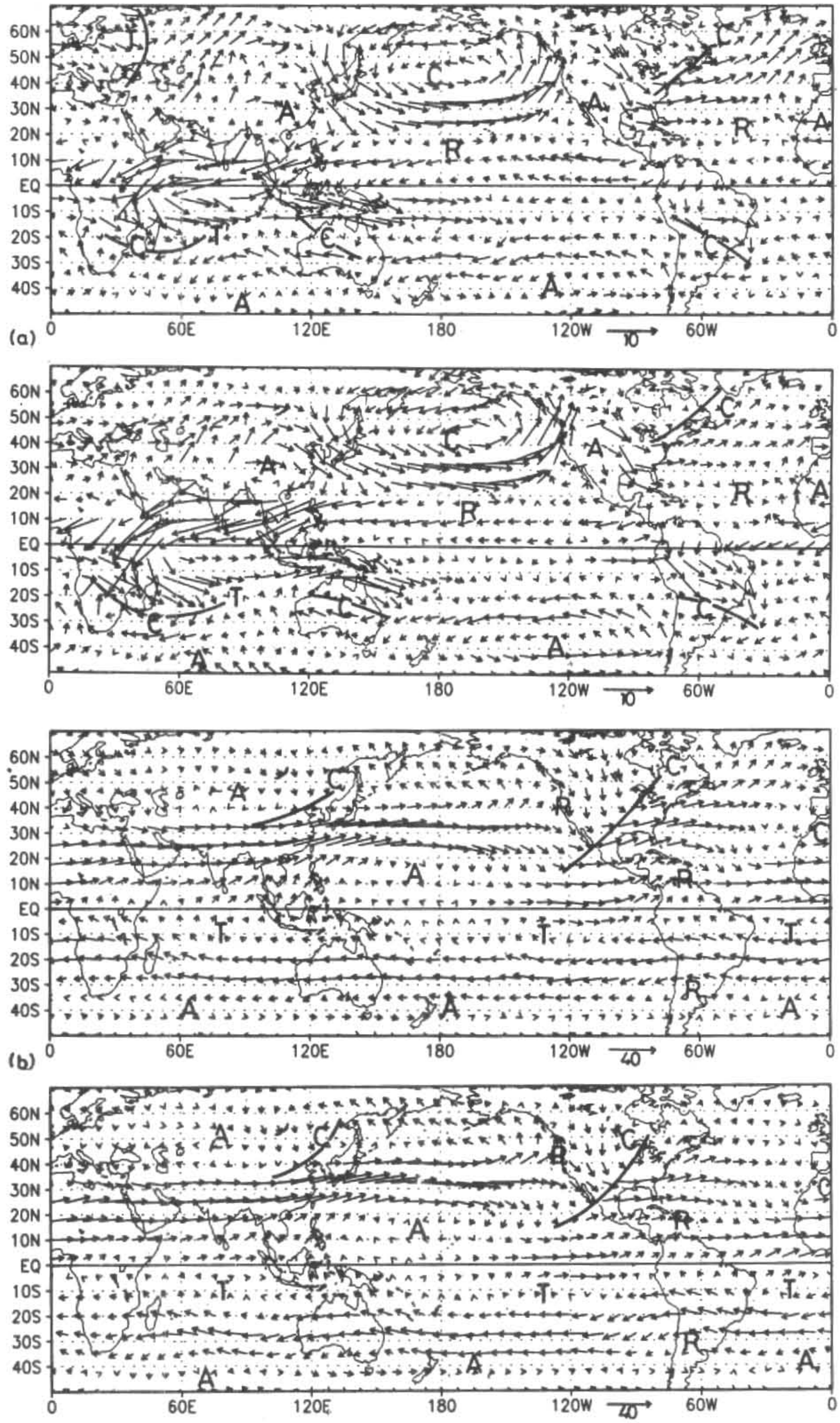

Figs.3(a&b). Global distributions of observed (reanalysis) and model wind anomaly vector (ms^{-1}) in January at (a) 850 hPa and (b) 200 hPa. Symbols denote: C- Cyclonic circulation; A- Anticyclonic Circulation; T-Trough and R- Ridge

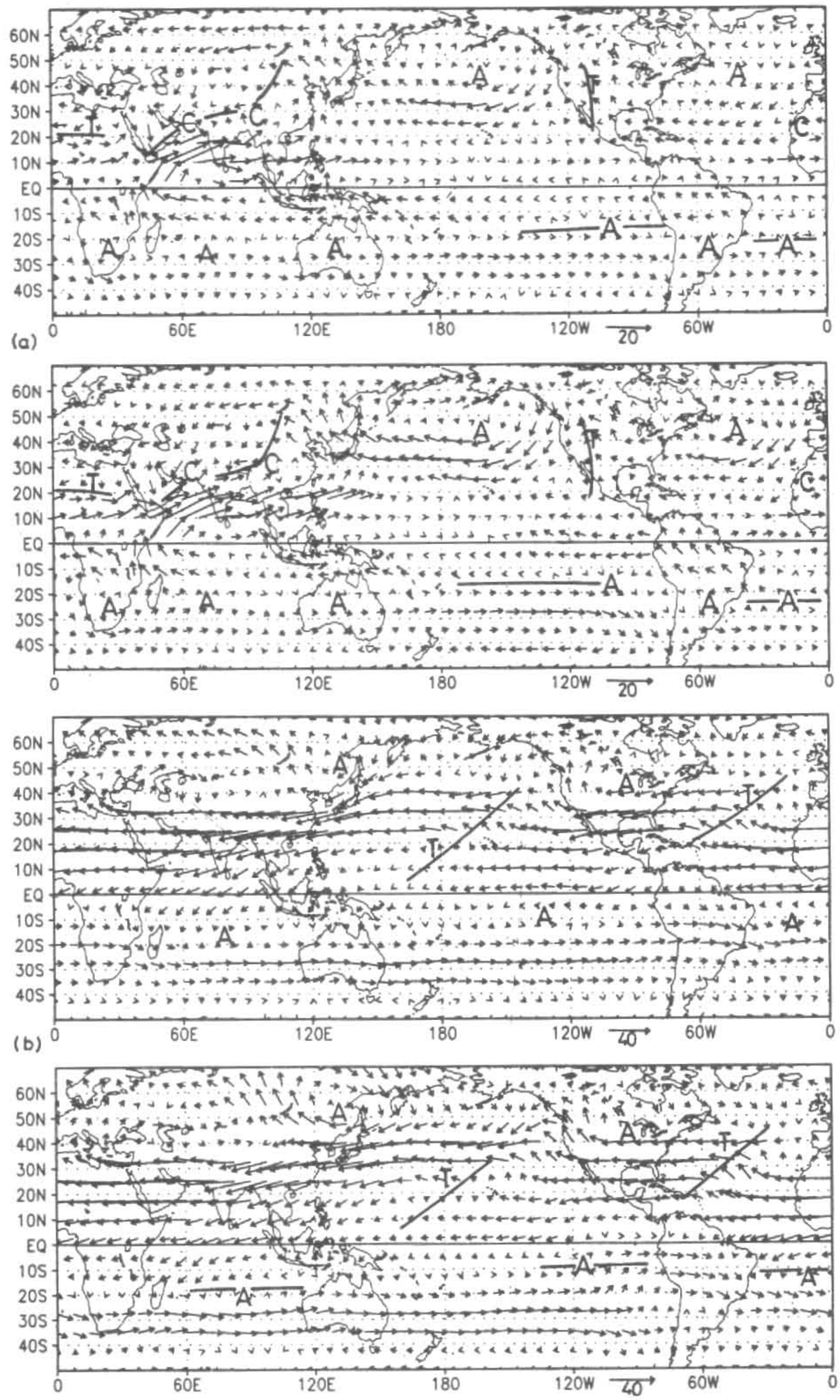

Figs.4 (a&b). Same as in Fig.3 but for July

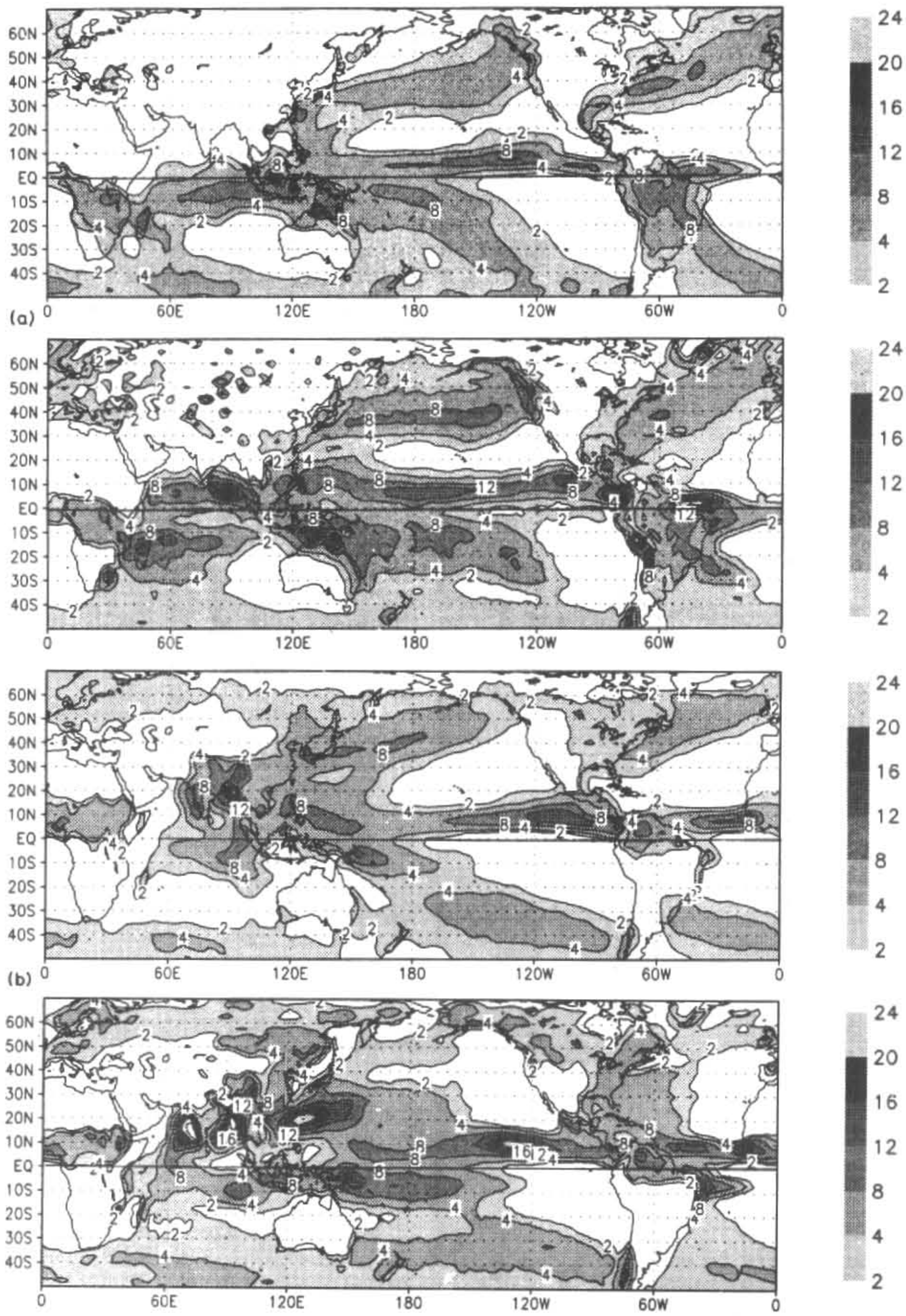

Figs.5(a&b). Global distributions of observed and model-generated total rainfall (mm/day): (a) January and (b) July. Areas with rainfall greater than 2 mm/day are shaded

estimated oceanic precipitation from Microwave Sounding Unit (MSU) measurements (Spencer, 1993). Model results which are used for comparison with reanalysis include mainly surface temperature and pressure, atmospheric circulation and rainfall but a few other parameters such as divergence, relative vorticity, vertical motion and Outgoing Longwave Radiation (OLR) are also used to aid our study.

3. Global distributions

The seasonal reversals of the fields of atmospheric temperature and pressure, wind and rainfall typical of monsoons can be revealed by an examination of the mean monthly values of these elements at the earth's surface. However, in the cases of temperature and pressure, a difficulty arises since the surface values which are measured at different elevations are required to be reduced to some

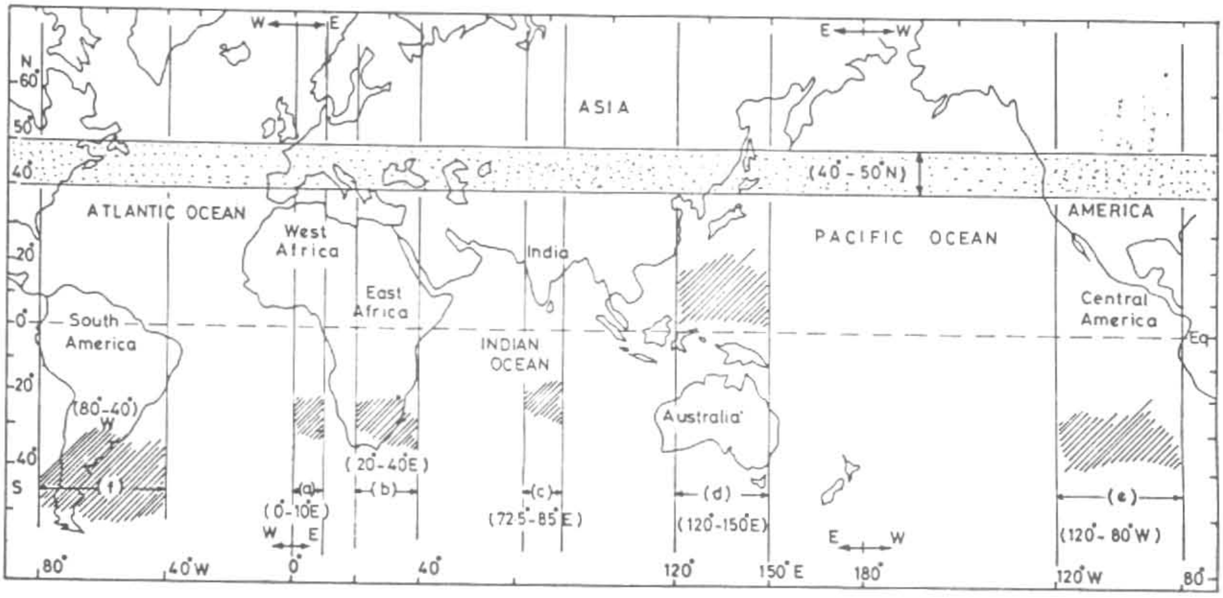

Fig.6. Selected longitudinal segments (hatched) of tropical regional monsoons and latitudinal segment (stippled) of extratropical monsoon

standard level such as the mean sea level. The procedure introduces errors, since atmospheric mass is artificially created or destroyed by it, as recently pointed out by Van Den Dool and Saha (1993). To avoid this difficulty, we worked with mean monthly anomaly (deviation of monthly mean from annual mean) values of these elements as measured at the surface (without reducing them to any other level) as well as other parameters used in our study. The only exception was in the case of rainfall where we used both mean and anomaly values. Our findings for the months of January and July when winter and summer monsoons reach their peak intensities are presented in the following subsections.

3.1. *Surface temperature anomaly*

Global distributions of observed and model surface temperature anomaly during January and July are presented in Figs. 1(a&b) respectively. In January (Fig.1a), the coldest (warmest) negative (positive) temperature anomalies are located over the continents in the northern (southern) hemisphere. The anomaly fields over the continents are reversed in July (Fig.1b). Major land-sea thermal contrasts between the continents and the oceans stand out in both the months in both north-south and east-west directions. The reversals of the temperature anomaly fields usually occur through the transition months April and October. It may be noted that a negative temperature anomaly appears in July in both observed and model climatology over the Arabian Sea and the equatorial belts of eastern Pacific and eastern Atlantic. This is due to the presence of cold ocean currents over these areas.

3.2. *Surface pressure anomaly*

The distributions of observed and model surface pressure anomaly for the months of January and July are shown in Figs.2(a & b) respectively. A comparison of the model with the observed anomaly patterns in January (Fig.2a) reveals a pattern correlation of 94.18% over the globe (90°N-90°S) and 96.12% over the tropics (20°N-20S). The corresponding pattern correlations in July (Fig.2b) are 94.01% over the globe and 96.10% over the tropics. Like surface temperature anomaly fields, surface pressure anomaly fields bring out in general the opposite phase relationship between the hemispheres as well as the contrast between the continents and the oceans.

In January (Fig.2a), consistent with the coldest (warmest) negative (positive) temperature anomaly over the continents in the northern (southern) hemisphere, the surface pressure anomaly is strongly positive (negative) over the continents in the northern (southern) hemisphere (except the Tibetan Plateau where it is negative). Strong pressure gradients are also noted between the continents and oceans in both the hemispheres. Over the oceans, some differences appear between the model and the observed distributions of surface pressure anomalies, especially over the northern hemisphere Pacific and Atlantic oceans. For example, the subtropical belt of high pressure along about 20°N, indicated by a positive anomaly, is continuous (broken) in the model but broken (continuous) in the observed distribution over the Pacific (Atlantic). Also, an area of negative anomaly of surface pressure associated with a deep low pressure

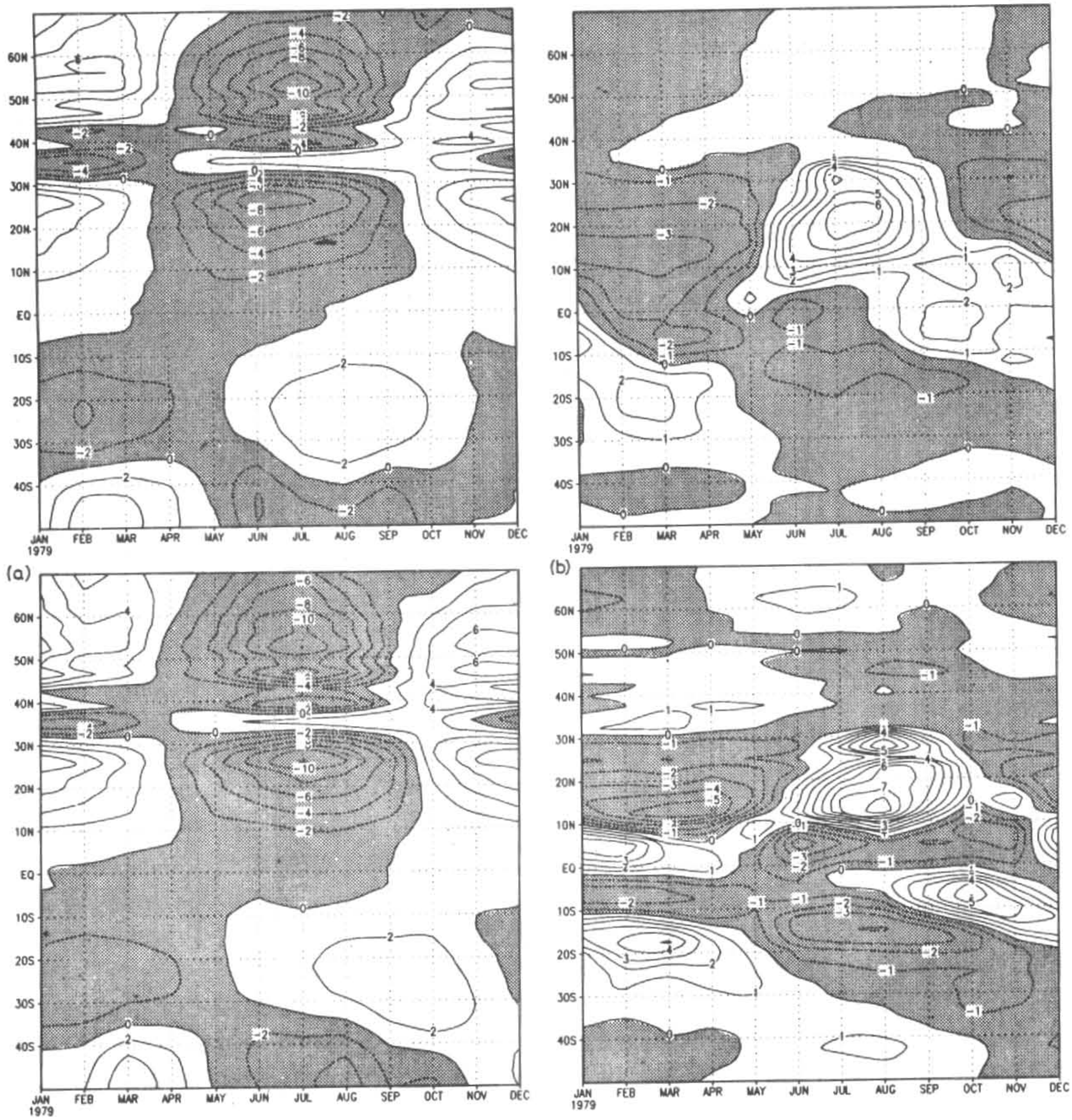

Figs.7(a&b). Latitudinal distributions of observed and model mean monthly anomaly of (a) surface pressure and (b) total rainfallof the wind over the selected longitudinal band of the Indian region. Sign convention for relative vorticity is same for both hemispheres: Positive- Anticlockwise, Negative- Clockwise

system over the north Pacific is deeper in the model than in the observed climatology. However, over the north Atlantic, the observed negative anomaly is deeper than the model anomaly. Elsewhere over the globe, there appears to be good agreement between the model and the observed distributions of surface pressure anomaly.

The entire surface pressure anomaly field, as described above, stands reversed in July (Fig.2b), with negative (positive) anomalies appearing over most of the continents in the northern (southern) hemisphere, except over the Tibetan Plateau, where a positive anomaly appears. The anomalous behaviour of the Tibetan Plateau (at average altitude near 4.5 km asl) in having a surface pressure anomaly opposite

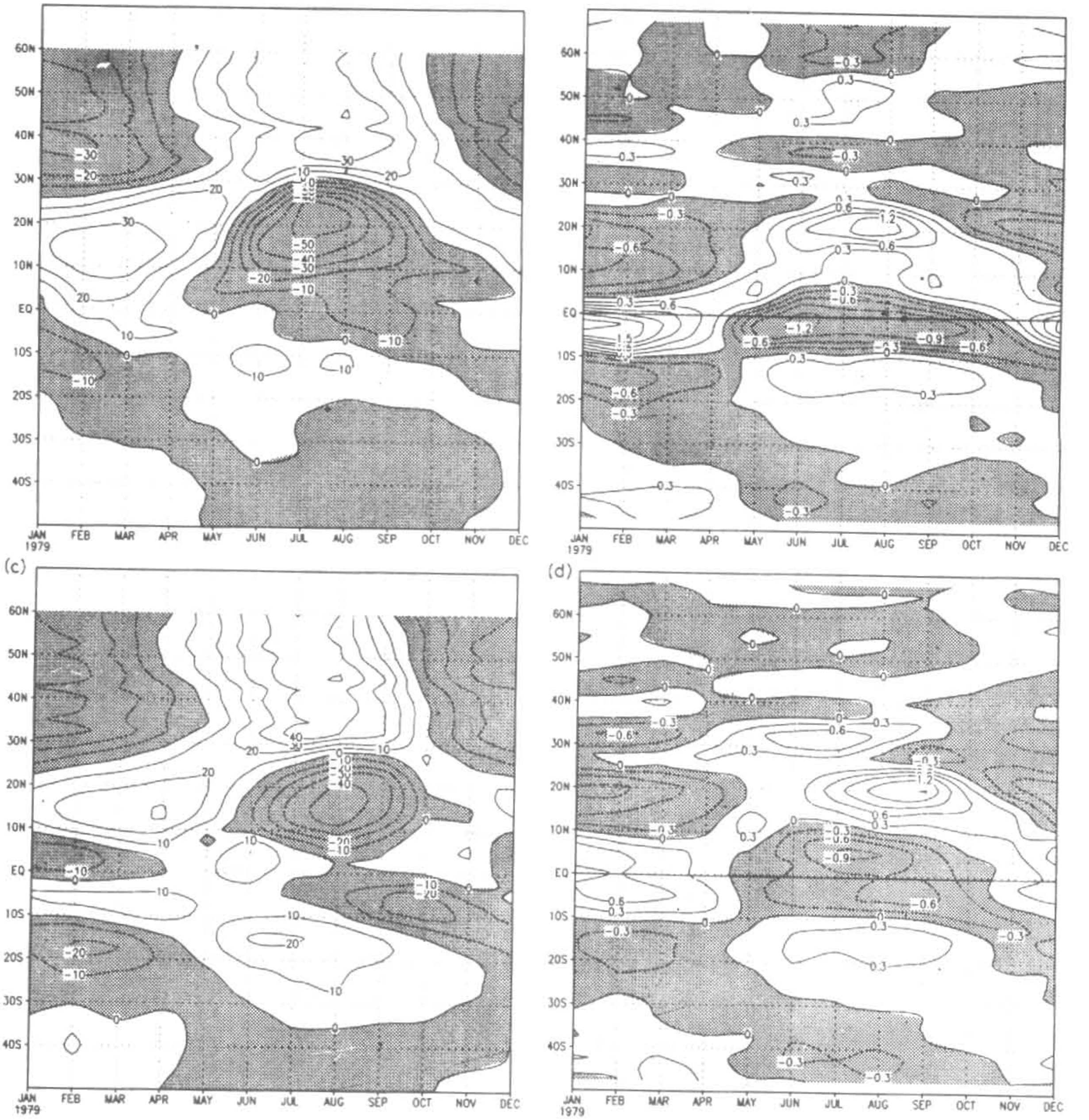

Figs.7(c&d). Latitudinal distributions of observed and model mean monthly anomaly of (c) OLR (Watts/square metre) and (d) 850 hPa relative vorticity (10^{-5} s^{-1}) of the wind over the selected longitudinal band of the Indian region. Sign convention for relative vorticity is same for both hemispheres: Positive- Anticlockwise, Negative- Clockwise

to that over its low-level surroundings in both January and July has been discussed by Saha *et al.* (1994) who attribute it mainly to the reversal of horizontal pressure pattern with height in both winter and summer monsoons.

3.3. *Atmospheric circulation*

Atmospheric circulation consistent with the distributions of surface temperature and pressure anomalies described in the foregoing subsections and its reversal with height and season appear to be well evident in observed and model circulations, not all of which can be presented and discussed here for lack of space. We, however, decide to present and discuss the circulation, using wind anomaly in vector form, at two pressure surfaces, *viz.*, 850 and 200 hPa only representing respectively the lower and the upper troposphere during January [Figs.3 (a & b)] and July Figs.4(a&b)].

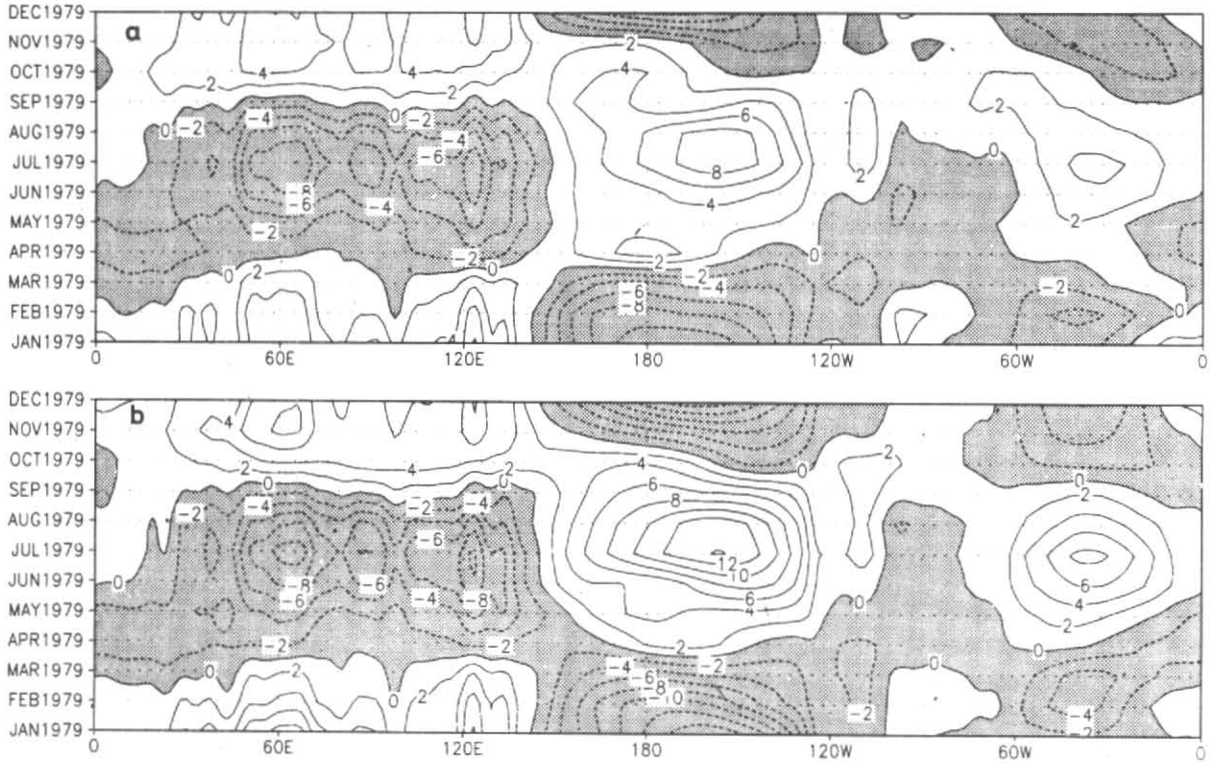

Figs.8(a&b). Longitudinal distribution of mean monthly anomaly of surface pressure (hPa) in the latitude band, 40°N-50°N, in different months: (a) Observed, (b) Model. Values are meridionally averaged over the latitude band. Negative values are shaded

Some noteworthy features of the circulations are:

(a) *January*

At 850 hPa during January (Fig.3a), wind systems diverging from anticyclones over cold continents in the northern hemisphere such as south Asia, north America and north Africa appear to cross the equator and converge into troughs of low pressure located over warm oceans near the equator and/or over warm continents in the southern hemisphere. In the Indian Ocean region where monsoon develops strongly, strong northeasterly trade winds diverging from an anticyclonic circulation over southern and eastern Asia appear to cross the equator and converge into an oceanic trough zone near the equator and into two continental trough zones, one over south Africa and the other over north Australia. Similar interhemispheric crossing and convergence into a trough zone in the opposite hemisphere is also evident over south America. Circulations over north Pacific and north Atlantic oceans are strongly cyclonic over the extratropics, anticyclonic over the subtropical belt and cyclonic near the equator.

In general, there appears to be a good measure of agreement between the observed and the model flow patterns over most parts of the globe. One may, however, note that a cyclonic circulation associated with a trough over western Asia does not appear in the model circulation. At 200 hPa during January (Fig. 3b), both observed and model circulations reveal two well-marked cyclonic troughs over the continents in the northern hemisphere, one over east Asia and the other over north America. Strong westerly (easterly) winds forming part of an anticyclonic circulation may be seen over the subtropical belt of the northern (southern) hemisphere. Over Pacific and Atlantic oceans, a weak cyclonic flow appears between the equator and about 10°S and an anticyclonic flow south of about 30°S. Large-scale cross-equatorial flow from the southern to the northern hemisphere appears to take place over the Indian Ocean and some of the continents in the equatorial zone. In general, there appears to be good agreement between the model and observed circulations.

(b) *July*

Atmospheric circulation at 850 hPa in July (Fig.4a) appears to be almost totally reversed in direction from that in January, with cyclonic circulations appearing, in general, over warm continents and anticyclonic circulations over

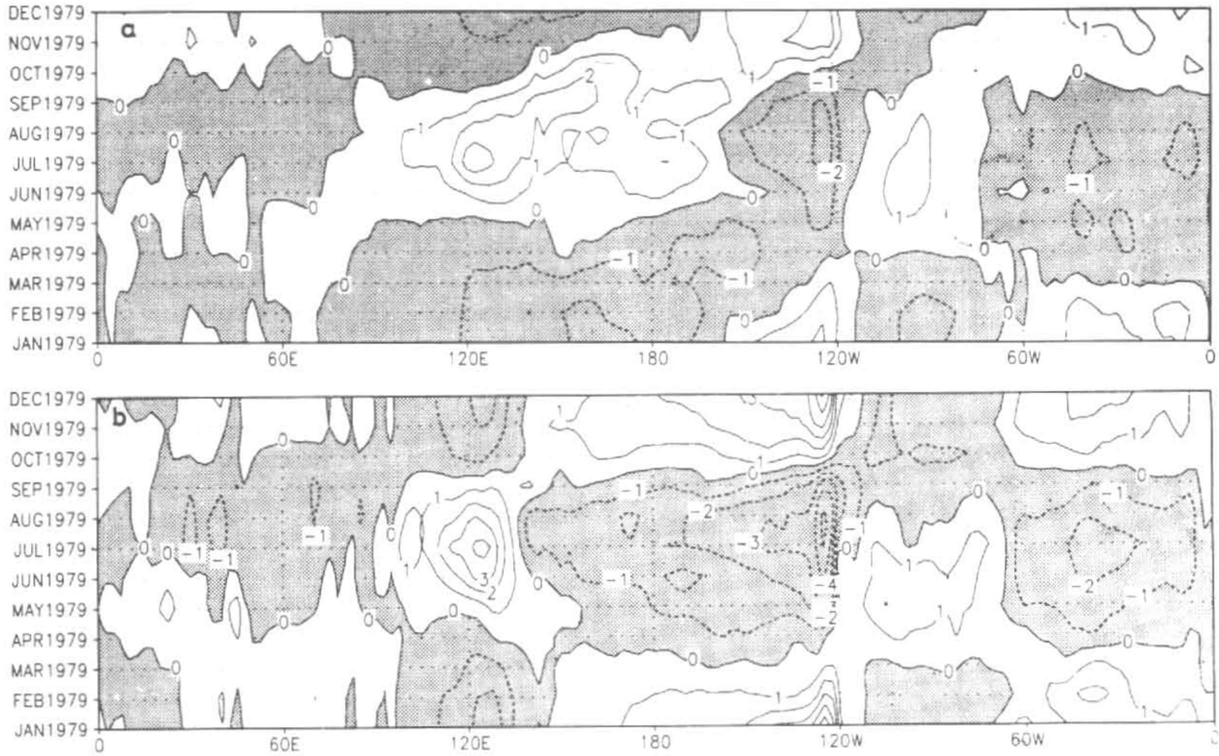

Figs.9(a&b). Same as in Fig.8 but for rainfall (mm/day)

cold oceans in the northern hemisphere. Over the Indian Ocean region, southeasterly trade winds diverging from the high pressure belt of the southern hemisphere with ridge along about 25°S cross the equator (mostly over the western part of the ocean) and converge as southwest monsoon into the low pressure trough zones over southern and eastern Asia. A weak cyclonic circulation over the western part of north and central America lies between two well- marked anticyclonic circulations centered over north Pacific and north Atlantic. Over south Pacific and south Atlantic, anticyclonic circulations appear with ridge along about 20°S.

Model and observed circulations appear to agree broadly over most parts of the globe. At 200 hPa during July (Fig.4b), the circulation in the northern hemisphere is dominated by two anticyclonic circulations, one over the northeastern part of Asia and the other over the northeastern part of north America. Two cyclonic troughs appear over mid-oceans of north Pacific and north Atlantic. Anticyclonic circulations also appear over the southern oceans with ridges along about 20°S over the Indian Ocean and 10°S over Pacific and Atlantic Oceans. In the northern hemisphere, strong easterly winds blow over the tropical belt, especially over tropical Indian Ocean where they also exhibit strong cross-equatorial flow.

3.4. *Rainfall*

The global distributions of observed and model-generated total rainfall during January and July are presented in Figs.5(a & b) respectively. Broad patterns detectable in them are the following:

(a) *January* (*Fig.5a*)

Except for north Pacific and north Atlantic oceans where large- scale rain falls in extratropical and equatorial belts (with a rainfall minimum in between over the subtropical belts), the northern hemisphere registers little rain in this month. Most of the rainfall is now in the southern hemisphere. Heavy falls are concentrated over south Africa, Australia and south America. In the Indian Ocean region, a prominent rainband extends from south Africa across the southern Indian Ocean towards the maritime continent where it overlaps with the rainband over northern Australia and joins up with the equatorial rainband over the Pacific.

Large-scale rainbands also appear along the south Pacific convergence Zone (SPCZ) and the south Atlantic Convergence Zone (SACZ). However, over several areas, the model-generated rainfall differs from observed rainfall. For example,

(*i*) In the Indian Ocean,, there is much more rain both north and south of the equator in the model than in observed climatology;

(*ii*) Much heavier rain is produced by the model in the ITCZ over the Pacific and the Atlantic than reported in the observations;

(*iii*) Midlatitude oceanic rainfall over the north Pacific and the north Atlantic covers wider areas and is more intense in the model than in the observations.

(b) *July* (*Fig.5b*)

At the seasonal extreme, the July rainfall distribution appears to be quite different from that during January. Major rainfall areas are now over the continents in the northern hemisphere. While the equatorial belts of the north Pacific and the north Atlantic continue to have rain (the rain belts appear to have shifted northward in July), the extensive rain over the extratropical belts of these oceans has dramatically diminished. On the other hand, the eastern seaboards of Asia and north America, which experienced little or no rain in January, are now considerably rainy. Australia is practically dry in July and most of the rainfall over Africa and south America occurs north of the equator. Considerable rain occurs over central America extending from near equator to almost 20°N.

In the Indian Ocean region, a feeble rainband appears a few degrees south of the equator, but the major rain areas are now over a wide stretch of land and sea extending northeastward from eastern Arabian Sea to Japan. However, little rain falls to the north and west of the Himalayas.

Rainband associated with the SPCZ is still well-marked and covers wide areas of the ocean eastward of Australia but that associated with the SACZ appears prominently in the model and it is hardly discernible in the observations. In July also, differences between the two rainfall climatologies appear over several areas. For example, *(i)* There is much heavier rain in the ITCZ and over western Pacific, maritime continent and southern and eastern Asia in the model than in the observations; *(ii)* Midlatitude oceanic rainfall over the north Pacific and the north Atlantic appears to be less intense in the model than in the observations; *(iii)* The subtropical dry belt over the south Pacific extends westward to about 140°W in the model but to almost 180°W in the observations; *(iv)* Similarly, in the north Atlantic, the subtropical dry belt extends from the African coast westward to about 40°W in the model but to almost 80°W in the observations.

4. Tropical and extratropical monsoons

The global distributions presented in the preceding section relate to two peak monsoon months, *viz*., January and July. They reveal little or nothing of the evolution of monsoon from month- to-month over any region. It may be interesting to study this evolutionary process for which we selected a few regions of the tropics, where monsoon moves in a north-south direction and a latitude-band in the extratropics where the movement appears to be largely in an east-west direction. These regions are shown in Fig.6. The evolution and movement in the two belts are studied separately for tropical and extratropical monsoons, using mean monthly anomaly values for the year 1979.

4.1. *Tropical monsoons*

To trace the seasonal north-south movement of the equatorial trough of low pressure and its associated ITCZ and rainbelt, we adopted the following approach:

We computed the mean monthly surface pressure anomaly values at all the latitudes along a longitude in any month and found the latitude where the anomaly value is negative and minimum. This latitude is likely to be the location of the equatorial trough in that month. In this way, one could trace the seasonal movement of the trough from month-to-month. The latitudinal movement of the associated rainbelt and OLR could also be traced in the same manner. we applied the method to the selected regions of the tropics (Fig.6), by zonally averaging the values of the parameter over the longitude band of the region along each latitude in each month of the year. The selected regions, alongwith the longitude bands, are:

(a) West Africa (0° - 10°E)

(b) East Africa (20°E - 40°E)

(c) India (72.5°E - 85°E)

(d) Australia (120°E - 150°E)

(e) North and central America (120°W - 80°W)

(f) South America (80°W - 40°W)

Our findings for each of the selected regions are summarized serially in the following. However, for lack of space, a typical example of the movement is discussed in respect of one region only, *viz*., India, where monsoon is known to develop strongly.

(a) *West Africa (0° - 10°E)*

The land-sea contrast with land to the north of about 5°N and sea to the south is dominant here. In both, observed and model surface pressure anomaly distributions, a negative value appears over the southeastern part of the southern Atlantic, between about 20°S and 30°S during the period

January to April. Towards the end of this period, there appears to be a tendency for this anomaly to move equatorward but there is little evidence that it actually crosses the equator. On the other hand a negative pressure anomaly located between 5°N and 10°N in March may have moved to about 15°N in April and 25°N in May. It remains along a mean latitude of about 25°N throughout the northern summer till September. Thereafter, it appears to move equatorward but there is little indication that it actually crosses the equator. The seasonal movement of the model-generated rainfall over west Africa appears to verify well against observed rainfall and OLR.

(b) *East Africa (20°E - 40°E)*

Unlike west Africa which has an ocean to its south, east Africa has a continuous landmass between about 30°N and 30°S. The land-sea contrast is practically absent here. There appears to be continuity in the movement of the equatorial trough, though, here also the field of negative surface pressure anomaly near the equator is rather flat and it is difficult to say with certainty that the trough moves from one hemisphere to the other. But the possibility of a single trough oscillating between the hemispheres and ushering in monsoons to northeast Africa in July and south Africa in January cannot be ruled out altogether. Model rainfall which appears to support such a possibility appears to be in agreement with observed rainfall and OLR.

(c) *India* (72.5°*E* - 85°*E*)

The geographical location of India at the southern periphery of the vast Asian continent with the extensive Indian Ocean to the south, perhaps, provides an ideal setting and maximum thermal contrast for development of a monsoon. Yet, the north-south seasonal movement of the equatorial trough appears to be rather complex and there is little suggestion from the observed and model field of mean monthly anomaly of surface pressure, which is quite flat in the equatorial region (Fig.7a), that a negative anomaly associated with the equatorial trough ever crossed the equator from the southern to the northern hemisphere to usher in the summer monsoon over India. However, a northward movement from about 10°N to about 25°N during June-July when monsoon reaches its peak intensity is clearly indicated.

Monsoon starts retreating from India in September and, by mid- October, reaches a latitude near 10°N. Further southward movement is not suggested by the field of surface pressure anomaly in the equatorial region which turns positive by end of October. It is not until two months later that an equatorial trough starts showing up over the southern Indian Ocean to begin the next monsoon cycle. Thus the question as to whether a single ET oscillates between the hemispheres to bring up the monsoon is not resolved by the field of mean monthly anomaly of surface pressure. We, therefore, examined the fields of rainfall, OLR, and relative vorticity of the wind [Figs.7(b-d)] for possible clue. Our findings are summarized as follows:

During both winter and summer, two separate equatorial troughs appear, one north and the other south of the equator, which are known to produce two separate belts of rain, low OLR and positive relative vorticity. The plausibility of the existence of two equatorial troughs over the Indian Ocean, one on each side of the equator, was first noted by Raman (1965). Several subsequent studies (Saha 1971 and 1973) appear to support Raman's findings.

(d) *Australia (120°E - 150°E)*

The land-sea distribution in this longitudinal band leads to development of a complex monsoon over the region. Between Australia in the south and eastern Siberia in the north lies a sizeable area of the western Pacific Ocean and the maritime continent which includes Philippines, New Guinea and some islands of Indonesia. Between November and February, the equatorial trough is located at a latitude of about 25°S over Australia. It starts moving northward in March and reaches a latitude near the equator by April. The field of negative surface pressure anomaly in the equatorial belt being flat about this time, it is just not possible to say whether any trough did or did not cross the equator. However, a prominent trough appears between about 30°N and 50°N around May and lasts till October. Considerable rainfall is associated with this midlatitude trough over the eastern seaboard of Asia during northern summer (Fig.5). This trough shows a southward movement after October but appears to lose its identity before it reaches about 15°N around November. A trough starts developing over Australia at this time to start the seasonal cycle. The observed distributions of rainfall and OLR over the region at different times of the year appear to support the model climatology.

(e) *North and central America (120°W - 80°W)*

An annual cycle of monsoon activity over this region, though considerably weaker than that over India or Australia, is largely due to land-sea thermal contrast that develops between the landmass of north and central America and the oceans that lie to the south. However, the mainland of north America with a wide longitudinal extent lies only north of about 30°N and the central America with its peninsular structure extending almost up to the equator contributes only feebly to land-sea thermal contrast in the north-south direction. The effect is clearly seen in the latitudinal distribution of mean monthly surface pressure anomaly which shows the northward movement of a feeble equatorial trough from a location near the equator during April-May. The trough reaches a latitude of about 35°N by early June and 40°N by July. It starts retreating thereafter and a steady southward movement follows till it reaches a latitude about 10°N by mid-October after which it disappears altogether. Model rainfall distribution appears to confirm the observation that the activity of the monsoon over this region is mainly confined to the northern hemisphere.

(f) *South America (80°W-40°W)*

In some respects, the land-sea configuration over this longitudinal belt appears to be opposite of that over the north American belt in that bulk of the ocean now lies to the north of the continent instead of the south. The equatorial trough over this region appears to be located at a mean latitude of about 30°S during November to March and then rapidly move northward to a latitude of about 15°N by April. Further northward movement appears to be prevented by a positive surface pressure anomaly to the north. The equatorial trough remains near the equator till September when it starts moving towards the south to reach a position near about 30°S by November. Model rainfall over the region appears to agree well with the observations.

4.2. *Extratropical monsoons*

To study the evolution of extratropical monsoons and their movements, we computed the latitudinal average of mean monthly surface pressure anomaly and rainfall over 10° latitude bands between 50°S and 70°N at all longitudes and studied the longitudinal distribution of the latitudinally-averaged values in different months.

The results relating to latitudinal band 40°N-50°N in both observed and model climatology are presented in Figs. (8 & 9) for surface pressure anomaly and rainfall respectively. Fig.8 brings out clearly the reversal of the surface pressure anomaly field between the continents and the oceans between summer and winter. In winter, the surface pressure anomaly is positive over the continents while it is negative over the oceans. The field reverses in summer with negative anomaly appearing over continents and positive over oceans. Fig.9 appears to show that a rainbelt associated with a minimum in surface pressure anomaly moves from ocean to continent during the months February to May and from continent to ocean during the months August to November. This type of longitudinal movement with reversal in the direction of movement between summer and winter appears to be a characteristic feature of extratropical monsoons and may be found over several regions, *e.g.*, between the Eurasian continent and the Pacific Ocean and between the north American continent and the Atlantic Ocean in the northern hemisphere and between the Australian continent and the Pacific Ocean in the southern hemisphere.

5. Conclusions

The present study, which examines the spatial and temporal anomaly (from the annual mean) of surface temperature and pressure as well as wind systems and rainfall in a 17-year mean climatology of the NCEP Global Forecast model and compares them with a 17-year mean observed climatology derived from NCEP's reanalysis finds that the essential features of the global monsoon circulation are simulated by the model fairly realistically over several regions of the globe in both tropical and extratropical latitudes.

The large diversity in the distribution of monsoons around the globe, in regard to their location, latitudinal extent and seasonal movement are well brought out by the model. In the case of tropical monsoons, a genuine doubt appears to exist regarding the concept of a single equatorial trough shuttling between the hemispheres in response to the seasonal oscillation of the sun across the equator to cause onset and retreat of monsoons.

Over most of the tropics, especially over warm oceans, there appears to be evidence of two equatorial troughs, one on each side of the equator and it is the equatorial trough in the summer hemisphere that appears to move and usher in the monsoon in that hemisphere while that in the winter hemisphere appears to mark time a few degrees on the other side of the equator.

In the extratropics, where large continents are flanked by oceans, there appears to be some evidence of an east-west seasonal movement of mean monthly surface pressure anomaly and rainfall between the continents and the oceans with the anomaly minimum and rainbelt migrating to the eastern seaboards of the continent during the summer and moving out to the ocean during the winter. This evidence would seem to strengthen the suggestion of an east-west monsoon circulation between the Asian continent and the Pacific Ocean. Our study finds evidence of similar east-west monsoon-type circulation over a few other regions as well, *e.g.*, between the north American continent and the Atlantic Ocean and between the Australian continent and the southern Pacific Ocean.

Acknowledgements

The authors' grateful thanks are due to the Director General of Meteorology, India Meteorological Department, for several facilities extended during the period of this study and to the anonymous reviewer whose valuable comments on an earlier version of the paper led to considerable improvement.

References

Grell, G.A., 1993, "Prognostic evaluation of assumptions used by cumulus parameterizations," *Mon. Wea. Rev.*, **121**, 764-787.

Kalnay, E., Kanamitsu, M., Kistler, R., Collins, W., Deaven, D. and Gandin, R., 1996, "The NCEP/NCAR 40- year reanalysis project," *Bull. Amer. Meteor. Soc.*, **77**, 437-471.

Kanamitsu, M., 1989, "Description of the NMC global data assimilation and forecast system", *Wea. Forecasting*, **4**, 334-342.

Kanamitsu, M., Alpert, J.C., Campana, K.A., Caplan, P. M., Deaven, D.G., Iredell, M., Katz, B., Pan, H.L., Sela, J. and White, G.H., 1991, "Recent changes implemented into the global forecast system at NMC," *Wea. Forecasting*, **6**, 425-435.

Krishnamurti, T. N., 1971, "Tropical east-west circulations during the northern summer," *J. Atmos. Sci.*, **28**, 1342-1347.

Krishnamurti, T.N., Kanamitsu, M., Koss, Walter James and Lee John, D., 1973, "Tropical east-west circulations during the northern winter", *J. Atmos. Sci.*, **30**, 780-787.

NOAA/NMC Development Division, 1988,, "Documentation of the NMC global model", (Available from NOAA/NCEP Environmental Modelling Center, 5200, Auth Road, Washington, D.C,, 20233, USA, 244p).

Pan, H.L. and Wan-shu Wu, 1994, "Implementing a mass flux convective parameterization package for the NMC medium-range forecast model", Preprints,, 10th Conf. on Numerical Weather Prediction, Portland, OR., Amer. Meteoro. Soc., 96-98.

Ramage, C.S., 1971, "Monsoon Meteorology," Academic Press, New York and London, 296 p.

Raman, C.R.V., 1965, "Cyclonic vortices on either side of the equator and their implications," *Proc. Sym. on Met. Results of the International Indian Ocean Expedition*, Bombay, July 22-26.

Saha, K.R. , 1971, "Cloud distributions over equatorial Indian Ocean as revealed by satellites," *Indian J. Meteor. Geophys.*, **22** , 389-396.

Saha, K.R., 1973, "Global distributions of double cloud bands over tropical oceans," *Quart. J. Roy. Meteor. Soc.* **99**, 551-555.

Saha, K.R., 1978,, "Some recent studies concerning tropical monsoons in India", *Proc. Sym. on Climatic Change and Food Production*, Univ. of Tokyo Press, Japan, 401-409.

Saha, K.R. and Saha, S., 1990, "Time-mean atmospheric circulation and diabatic heating over the Arabian sea during July," *Mausam*, **41**, 21-30.

Saha, K.R., Van den Dool, H.M. and Saha, S., 1994, "A note on the annual cycle in surface pressure on a plateau compared to its surroundings," *J. Climate*, **7**, 2014-2019.

Spencer, R.W., 1993, "Global oceanic precipitation from the MSU during 1979-91 and comparisons to other climatologies," *J. Climate*, **6**, 1301-1326.

Van Den Dool, H.M. and Saha, S., 1993, "On the seasonal redistribution of atmospheric mass in a 10-year GCM run," *J. Climate*, **6**, 22-30.